INDC (FR) 9/L
NEANDC (E) 174"L"

COHERENT OPTICAL AND STATISTICAL MODEL CALCULATIONS OF NEUTRON CROSS SECTIONS FOR ^{238}U BETWEEN 1 keV AND 20 MeV

J. JARY, Ch. LAGRANGE, P. THOMET

Service de Physique Nucléaire, Centre d'Etudes de Bruyères-le-Châtel
B.P. n° 561 - 92542 Montrouge - France -

February 1977

COMMISSARIAT A L'ENERGIE ATOMIQUE

FRANCE

- CONTENTS -

Jacqueline JARY, Christian LAGRANGE, Paul THOMET

COHERENT OPTICAL AND STATISTICAL MODEL CALCULATIONS OF NEUTRON CROSS-SECTIONS FROM ^{238}U BETWEEN 1 keV AND 20 MeV

J. JARY, Ch. LAGRANGE, P. THOMET

Service de Physique Nucléaire
Centre d'Etudes de Bruyères-le-Châtel
B.P. n° 561 - 92542 Montrouge - France -

ABSTRACT

We present a coherent method of calculation for a set of neutron nuclear cross sections in the energy range 1 keV - 20 MeV using the optical and statistical model. This method is applied to neutron interactions with ^{238}U. The choice of experimental constraints leading to the determination of the various model parameters is presented and discussed. We have obtained a coherent optical and statistical parameter set which can be extrapolated easily and with great confidence for complete and accurate calculations of neutron cross sections in this mass region.

METHODE DE CALCUL COHERENTE DES SECTIONS EFFICACES NEUTRONIQUES DE L'URANIUM 238 DE 1 keV A 20 MeV PAR LES MODELES OPTIQUE ET STATISTIQUE

RESUME

Nous présentons une méthode de calcul cohérente d'un ensemble de sections efficaces neutroniques dans le domaine d'énergie 1 keV - 20 MeV, utilisant les modèles optique et statistique. Cette méthode est appliquée à l'Uranium 238. Le choix des données expérimentales servant à la détermination des divers paramètres des modèles est discuté. La paramétrisation cohérente obtenue peut être aisément extrapolée pour des calculs complets et précis des sections efficaces neutroniques de cette région de masse.

I - INTRODUCTION

Successful technology of nuclear reactor requires accurate knowledge of the neutron cross sections of uranium isotopes. We describe a method to obtain with great accuracy and easy extrapolation complete calculated values of these neutron cross sections.

This paper presents an application of this method to the calculation of direct and compound reaction cross sections of ^{238}U over the incident energy range 10 keV to 20 MeV.

In this work, the total, the shape elastic and direct inelastic scattering cross sections were obtained using an original method of parameterization of the deformed optical potential. An improved version of the coupled-channel code "JUPITOR 1" [1] provided the numerical results. The generalized neutron penetrabilities resulting from these calculations were introduced into our statistical model codes which describe the compound nuclear reactions such as compound elastic and inelastic scattering, radiative capture, fission, (n,2n) and (n,3n) reactions. We give the excitation functions of all the above cross sections. Moreover some angular distributions are shown for elastic scattering and for direct inelastic scattering to the 2^+ and 4^+ states.

The formalism of the optical and statistical models used in the present calculations is recalled in section II. The section III describes how our procedure for determinating the model parameters is based on some carefully selected experimental data (strength functions, total and fission cross sections). The results from the application of this procedure to ^{238}U are given in section IV. The overall good agreement obtained between the present coherent calculations and the available ^{238}U experimental data is presented and discussed in section V.

It is reasonable to hope that the same theoretical procedure can be applied with confidence to the calculation of the neutron cross sections of less well known neighbouring nuclei for which requests have been made.

II - FORMALISM

II-1- General formulation

Since the ^{238}U nucleus exhibits a high degree of deformity as shown by the low-lying collective states of its discrete spectrum, the neutron interactions must be analyzed in terms of a deformed optical potential, that is by the coupled-channel model.

Differential shape elastic, direct inelastic and total cross-sections are obtained in the usual way by solving the Schrödinger equation with the Hamiltonian

$$H = H_T + T + V(r,\theta,\varphi) \qquad (1)$$

T and H_T are respectively the kinetic energy of the relative motion and the Hamiltonian of the target.

The generalized local optical potential $V(r, \theta, \varphi)$ takes the form

$$V(r,\theta,\varphi) = -Vf(r,a,R) + 4iW\left(\frac{d}{dr}\right) f(r,a',R') + \left(\frac{\hbar}{m_\pi c}\right)^2 \vec{\sigma}.\vec{L}\; V_s\left(\frac{1}{r}\right)\left(\frac{d}{dr}\right) f(r,a,R) \qquad (2)$$

The quantities r, θ, φ are the body-fixed coordinates, and the radii R and R' depend on the angle θ, deformation parameters β_2, β_4 and mass number A as follows :

$$\begin{aligned} R &= r_0 A^{\frac{1}{3}} \left[1 + \beta_2 \; Y_{20}(\theta) + \beta_4 \; Y_{40}(\theta)\right] \\ R' &= r'_0 A^{\frac{1}{3}} \left[1 + \beta_2 \; Y_{20}(\theta) + \beta_4 \; Y_{40}(\theta)\right] \end{aligned} \qquad (3)$$

The function $f(r,a,R)$ was taken to have the Saxon-Woods form

$$f(r,a,R) = \left[1 + \exp\left(\frac{r-R}{a}\right)\right]^{-1} \qquad (4)$$

The potential was expanded in Legendre polynomials up to order $\lambda = 8$. The formalism employed here is based on the coupled channel model developed by T. Tamura [1]. For neutron energies high enough ($E \gtrsim 10$ MeV), the so-called adiabatic approximation was assumed. At lower energies, in a first approach, the ground state and the first excited state coupling scheme (0^+, 2^+) was employed ; in a second approach, a larger coupling scheme (0^+, 2^+, 4^+) was taken.

The compound nuclear processes were calculated using the statistical theory for the decay of the compound nucleus [2]. In the energy range below 2 MeV, the reaction cross sections are derived from the formalism of Moldauer [3] (statistical model with angular momentum and parity conservation and fluctuation correction) whereas at higher energy they are calculated using a spin-independent statistical model [4].

Following Moldauer, the reaction cross section is written

$$\sigma_{cc'}^{J\Pi}(E) = \pi \lambda\!\!\!^{-}{}_c^2 \left[\left\langle \frac{\theta_c(E)\ \theta_{c'}(E)}{\theta(E)} \right\rangle - \frac{1}{4}\,\delta_{cc'}\ Q_c^{J\Pi}(E)\ \langle \theta_c(E) \rangle_{J\Pi} \right] \tag{5}$$

where the indices c and c' label the set of quantum numbers of the partial waves in the entrance and exit channels respectively ; E is the incident neutron energy, and $J\Pi$ are the spin and parity of the compound nucleus. Moreover :

$$\langle \theta_c(E) \rangle_{J\Pi} = \left[\frac{2}{Q_c^{J\Pi}(E)} \right] \left[1 - \left(1 - T_c(E,J\Pi)\, Q_c^{J\Pi}(E) \right)^{\frac{1}{2}} \right] \tag{6}$$

In this equation $T_c\,(E,J\Pi)$ is a transmission coëfficient and $Q_c^{J\Pi}$ is the statistical fluctuation parameter ($0 \leqslant Q_c^{J\Pi} \leqslant 1$) [3].

The ratio $\langle\theta_c(E)\theta_{c'}(E)/\theta(E)\rangle_{J\Pi}$ is given by the fluctuation correction factor $F_{cc'}^{J\Pi}(E)$:

$$F_{cc'}^{J\Pi}(E) = \frac{\langle \theta_c(E)\,\theta_{c'}(E)/\theta(E) \rangle_{J\Pi}}{\langle \theta_c(E) \rangle_{J\Pi} \langle \theta_{c'}(E) \rangle_{J\Pi} / \langle \theta(E) \rangle_{J\Pi}} = \int_0^{\infty} \frac{(1 + 2\,\delta_{cc'})\,dt}{F_c^{J\Pi}(E,t)\,F_{c'}^{J\Pi}(E,t)\,\prod_{c''}\left[F_{c''}(E,t)\right]^{\nu_{c''}/2}} \tag{7}$$

In equation (7) ν_c is the number of degrees of freedom in the c channel, and $f_c^{J\Pi}(E,t)$ is the relative contribution of the same channel :

$$F_c^{J\pi}(E,t) = 1 + \frac{2t}{\nu_c}\left[\frac{\langle\theta_c(E)\rangle_{J\pi}}{\sum_{c'}\langle\theta_{c'}(E)\rangle_{J\pi}}\right] \tag{8}$$

II-2- Fission cross sections

For incident energies below 2 MeV the individual fission channel characteristics have to be taken into account. Then, the total fission cross section is calculated as in ref. [5]

$$\sigma_{n,f}(E) = \sum_{JK\pi} \sigma_c(E,J\pi) \cdot B(E,JK\pi) \tag{9}$$

and the differential fission cross section with fragment direction Θ relative to the incident beam direction is given by

$$\sigma_{n,f}(E,\Theta) = \sum_{J\pi}\sum_{KM} \sigma_c(E,J\pi) \cdot B(E,JK\pi)\, W^J_{MK}(E,\Theta) \tag{10}$$

with $\quad W^J_{MK}(E,\Theta) = \frac{1}{4}(2J+1)\left|\, d^J_{MK}(\Theta)\right|^2$

In these expressions $\sigma_c(E,J\Pi)$ is the cross section for formation of the compound nucleus of total spin J and parity Π., deduced from the coupled channel calculations. $B(E\,;\,JK\Pi)$ is the fission branching ratio corrected for the fluctuation factor (cf eq. (7))

$$B(E,JK\pi) = \frac{T_f(E,JK\pi)\quad F_{n,f}^{JK\pi}(E)}{\sum_{K\leq J} T_f(E,JK\pi) + T_n(E,J\pi) + T_\gamma(E,J\pi)} \tag{11}$$

Here, K and M are the components of the nuclear spin along the symmetry axis and the incident beam direction respectively. The function $d^J_{MK}(\theta)$ is the reduced rotational wave function describing the orientation of the nucleus at the saddle point.

The fission transmission coefficients $T_f(E,JK\Pi)$ are obtained by solving the Schrödinger equation with a two-humped fission deformation potential constructed on three connected parabolas [Fig. 1]. In the first well, full damping is assumed. In the second well, the damping of the vibrational levels into the intrinsic excited states is phenomenologically described by a complex potential [5]. The detailed calculation of the γ-ray ($T\gamma(E,J\Pi)$), neutron ($T_n(EJ\Pi)$), and fission ($T_f(E,JK\Pi)$) transmission coefficients is given in Appendix.

Over the incident energy range 2-20 MeV the total fission cross section has been written [6]

$$\sigma_{n,f}(E) = \sum_{x=0}^{x=3} \sigma(n,xnf) \tag{12}$$

where $\sigma(n,xnf)$ is the fission cross section after evaporation of x neutrons from the compound nucleus. Within the spin-independent statistical model we have used in this energy range :

$$\sigma(n,xnf) = \sigma_c(E)\,\frac{\Gamma_n(E_c)}{\Gamma_n(E_c)+\Gamma_f(E_c)+\Gamma_\gamma(E_c)}\,P(E_c,xnf) \tag{13}$$

The compound nucleus formation cross section $\sigma_c(E)$ is obtained as the sum of partial quantities $\sigma_c(E,J\Pi)$ (cf eq. (9)) on all the available compound nucleus states ($J\Pi$). The second factor in equation (13) is the neutron branching ratio. The partial widths $\Gamma_n(E_c)$, $\Gamma_f(E_c)$ and $\Gamma\gamma(E_c)$ are also given in Appendix. $P(E_c,xnf)$ is the relative probability that the compound nucleus at excitation energy E_c emits x neutrons and then fissions. For $x>1$:

$$P(E_c,xnf) = \frac{\displaystyle\int_0^{E_c-(S_1+S_2+\dots+S_x)} \varepsilon.\,\sigma_c(\varepsilon)\,\rho(E_R)\,\frac{\Gamma_n(E_R)}{\Gamma_n(E_R)+\Gamma_f(E_R)+\Gamma_\gamma(E_R)}.\,P\left[E_R,(x-1)nf\right]d\varepsilon}{\displaystyle\int_0^{E_c-S_1} \varepsilon\,\sigma_c(\varepsilon).\,\rho(E_R)\,d\varepsilon} \tag{14}$$

In these expressions ε is the centre-of-mass kinetic energy of the exit neutron channel ; $\sigma_c(\varepsilon)$ is the inverse reaction cross section equal to the compound nucleus formation cross section ; $\rho(E_R)$ is the level density in the residual nucleus at excitation energy E_R ; S_1, $S_2 \ldots S_x$ are the neutron separation energies for, respectively, the compound nucleus, the first residual nucleus, and so on. $\Gamma_n(E_R)/[\Gamma_n(E_R) + \Gamma_f(E_R) + \Gamma_\gamma(E_R)]$ and $P[E_R,(x-1)nf]$ have the same meanings as those used in equation (13), but for the residual nucleus. For $x = 1$, the last residual nucleus can only fission, so :

$$P(E_c, nf) = \frac{\displaystyle\int_0^{E_c - S_1} \varepsilon . \sigma_c(\varepsilon) \cdot \rho(E_R) \cdot \frac{\Gamma_f(E_R)}{\Gamma_n(E_R) + \Gamma_f(E_R) + \Gamma_\gamma(E_R)} \, d\varepsilon}{\displaystyle\int_0^{E_c - S_1} \varepsilon . \sigma_c(\varepsilon) \; \rho(E_R) \, d\varepsilon} \qquad (15)$$

II-3- Radiative capture cross section

We here neglect the direct and semi-direct radiative capture phenomena. Then, following equation (5), we use in the energy range 1 keV - 2 MeV :

$$\sigma_{n,\gamma}(E) = \sum_{J\pi} \sigma_c(E, J\pi) \, P_\gamma(E, J\pi) \, F^{J\pi}_{n,\gamma}(E) \qquad (16)$$

In this expression $F^{J\Pi}_{n,\gamma}(E)$ is given by equation (7), $P\gamma(E, J\Pi)$ is the γ-ray branching ratio :

$$P_\gamma(E, J\pi) = \frac{T_\gamma(E, J\pi)}{\sum_K T_f(E, JK\pi) + T_n(E, J\pi) + T_\gamma(E, J\pi)} \qquad (17)$$

II-4- Compound inelastic and (n,xn) cross sections

The inelastic neutron cross section relative to the target nucleus left in an excited state λ (energy E_λ, spin I_λ, parity Π_λ) is written, from equation (5) :

$$\sigma_{n,n'_\lambda}(E) = \sum_{J\pi} \sigma_c(E,J\pi)\, P_\lambda(E,J\pi)\, F^{J\pi}_{n,n'_\lambda}(E) \qquad (18)$$

with the branching ratio

$$P_\lambda(E,J\pi) = \frac{T_{n(\lambda)}(E-E_\lambda, J\pi)}{\sum_K T_f(E,JK\pi) + T_n(E,J\pi) + T_\gamma(E,J\pi)} \qquad (19)$$

$F^{J\Pi}_{n,n'_\lambda}(E)$ is given by equation (7). Following the expression for the neutron transmission coefficient $T_{n(\lambda)}(E-E_\lambda,J\Pi)$ (see Appendix), the target exit state can be a discrete or a continuous excited state.

For incident energies higher than 2 MeV, the spin-independent statistical model is used. As for fission (equation (13)), we use :

$$\sigma(n,xn) = \sigma_c(E) \cdot \frac{\Gamma_n(E_c)}{\Gamma_n(E_c) + \Gamma_f(E_c) + \Gamma_\gamma(E_c)} \cdot P(E_c, xn) \qquad (20)$$

$$(x = 1,2,3,)$$

All terms of this equation have the same meanings as those of equation (13) except for $P(E_c,xn)$ which represents the relative probability that the compound nucleus at excitation energy E_c emits x neutrons and then decays by γ-emission. For $x>1$, $P(E_c,xn)$ is identical to $P(E_c,xnf)$ (cf. equation (14)). For $x = 1$ we have here :

$$P(E_c, n) = \frac{\displaystyle\int_0^{E_c-S_1} \varepsilon\, \sigma_c(\varepsilon)\, \rho(E_R)\, \frac{\Gamma_\gamma(E_R)}{\Gamma_n(E_R)+\Gamma_f(E_R)+\Gamma_\gamma(E_R)}\, d\varepsilon}{\displaystyle\int_0^{E_c-S_1} \varepsilon\, \sigma_c(\varepsilon)\, \rho(E_R)\, d\varepsilon} \qquad (21)$$

III - PARAMETER DETERMINATION PROCEDURES

III-1- Coupled channel optical model

Cross section calculations were performed with a revised version [7] of the coupled channel computer code "Jupitor-1" written by T. Tamura. We thought that the generalized optical model with a unique and physically coherent parameter set was able to reproduce neutron data at low energies as well as not too high energies (10 keV to 20 MeV for example). As neutron energies are increased from a few keV to several MeV, calculated values become less and less sensitive to variation of optical parameters or to the chosen coupling scheme. At low energies, the s and p-wave strength functions are related through calculated transmission coefficients to the compound nucleus formation cross section and thus to the imaginary part of the potential. Moreover, the shape elastic cross section (σ_e) can be related at very low energy to the experimental value of the potential scattering radius ($\sigma_e = 4\pi R'^2$). The total cross section is the only calculated cross section directly comparable throughout the full energy range to energy average measurements. For these reasons, we have adopted here a new procedure for determining the optical model parameters. We require first that we have satisfactory fits to the experimental values of s and p-wave strength functions and potential scattering radius. The parameter set so obtained is used to compute the total cross section up to a few MeV, and so we deduce the energy variation of the depths of the real and imaginary potential wells. The optical model parameters have so been constrained to give good agreement with the experimental values of strength functions, scattering radius and total cross section over the full energy range. Above 3 MeV, it is almost impossible for ^{238}U to distinguish between the elastic and inelastic scattering to the first excited states. We will compare the experimental results to calculated values obtained by summing differential scattering to the nuclear states included in the coupling scheme with energies less than 400 keV.

Remark

Various experimental methods were used to obtain strength functions and scattering radius, for example the analysis of resolved resonance data and the analysis of average total cross section data from a few keV to the MeV region. We have chosen to make comparisons between the calculated values and the experimental results obtained from the R matrix theory analysis of the average total cross sections as was done by Uttley [8]. There has been a great number of measurements of the total neutron cross sections, so we have made comparisons between calculated results and data extracted from the Evaluated Nuclear Data File (ENDF/BIV).

III-2- Statistical model parameters

In the presence of fission competition, statistical model calculations are based on an adjustment to various experimental fission data.

To calculate the fission transmission coefficients (equations (11), (17) and (19), the fission energy, spins and parity (E_A, J, K, Π) of the fission channels must be found by fitting calculated fission characteristics to the known experimental values.

The data which are used to fix the fission parameters by the method of the least-squares are :

- The total fission cross-section : $\sigma_{n,f}$ (E) (equation (9))
- The differential fission cross section : $\sigma_{n,f}$ (E,Θ) or $\sigma_{n,f}(E,\Theta)/\sigma_{n,f}(E,90°)$ (equation (10))
- The anisotropy of fission fragments (equation (10)) :

$$a_s(E) = W(E,0^\circ) / W(E,90^\circ) \tag{22}$$

- The g_ℓ coefficients of the Legendre polynomial expansion :

$$\sigma_{n,f}(E,\Theta) = \sum_\ell g_\ell(E) \; P_\ell(\cos\theta) \tag{23}$$

At neutron incident energies below 2 MeV, the following parameters have been adjusted to obtain good agreement with the total fission cross section :

a) Heights of the fission barriers for the exit channels which are considered in the calculations. For each (J,K,Π) channel, the shape of the barrier (three connected parabolas) is chosen and remains unchanged (fig. 1) ($E_A - E_2$ = constant, $E_B - E_2$ = constant), but the overall position is adjusted.

b) The effective number of fission channels N_f (K,Π) (equations (A14) and (A15)). This parameter is adjusted to take into account the effect of other channels having the same (J,K,Π), but situated higher in energy. We must note that the cross section of non-fissile nuclei is more sensitive to the heights of the fission channels than to their effective number in the lower part of incident neutron energies. At higher energy, as the total fission cross section increases very rapidly, the effective number of fission channels becomes the important parameter to adjust. The imaginary potential W_m can be deduced from photofission anisotropies. In this work, calculations have been performed assuming full damping.

At neutron incident energies higher than 2 MeV the coefficients K1 and C (equations (A16) and (A17) of Appendix) are the adjustable parameters to fit the total fission cross section. The shape of the first-chance plateau of fission (2 MeV - 6 MeV) determines the K1 and C coefficients of the compound nucleus, the one of the second-chance plateau of fission, those of the first residual nucleus, and so on. The simplified expressions used for the fission widths and level densities together with the incertitude about the heights of the equivalent single fission barriers involve some ambiguity between the K1 and C parameters.

After the determination of the transmission coefficients, fission, radiative capture, compound inelastic, elastic and (n,xn) cross sections are obtained from equations (9), (10), (12), (16), (18) and (20).

Over the full range of incident energies there is an interdependence between the barrier characteristics and the level densities. In the present work, the heights and effective number of fission channels are determined assuming, firstly, a definite shape for the barriers, and secondly, Fermi-gas and constant temperature level densities [9] with associated parameters (shell correction and pairing energy for instance). At higher energy the equivalent single fission barrier characteristics are taken from experiment, and the coefficients (such as K_1 and C) related to level densities are adjusted to fission cross sections.

IV - APPLICATION TO ^{238}U

IV-1- Coupled channel optical model parameters

We have noted that at low energies the total parameterisation was very sensitive to the choice of nuclear deformation parameters. For this reason, and because of large experimental errors associated with the measurements, we have chosen deformation parameters derived from calculations based on the Nilsson model and the method of Strutinsky as described by Möller [10]. The values are the following : $\beta_2 = 0.216$, $\beta_4 = 0.067$. The choice of optical model parameters is not independent of the choice of the coupling basis, so we present two sets of parameters (cf. Table 1) determined by the same procedure (Chap. III) using the two coupling bases (0^+, 2^+) and (0^+, 2^+, 4^+). In each case, the radial factors of the coupling terms were taken as real, and the coupling potential was the same for all the channels and related to the diagonal potential. Although agreement was obtained in both cases for the strength functions and the scattering radius (cf. Table 2), a good agreement for the total cross sections (cf. Figures 2a, 2b) was only obtained with the larger coupling basis (0^+, 2^+, 4^+). Experimental values of the total cross sections were extracted from references [11, 12]. To complete the comparison of total cross sections results, we mention that in the range of energies 30 keV to 10 MeV, the calculated values (using the 0^+, 2^+, 4^+ coupling basis) are very close to the recommended values of the experimental evaluation of Smith [13]. Figures 2c and 2d show the comparisons at 4 and 5.54 MeV of calculated and measured "elastic" angular distributions. Since there has been no systematic redetermination of the parameters, these last results permit us to judge the adequacy of the parameterisation. Here again a better agreement is obtained with the larger coupling basis and the associated optical parameters. The various measurements reproduced here have been taken from references [14, 15, 16, 17]. In order to demonstrate the influence of optical parameters on calculated values of strength functions and scattering radius, calculations were performed using the 0^+, 2^+, 4^+ coupling basis with small variations of parameters shown in Table 1. The modified parameters and corresponding results are presented in Table 3 ; initial values are in the first column, in the second and third columns only V was varied, in the fourth column W and a' were varied so that the product Wa' remains constant ; in the last column V_s was put equal to zero. These results explain the practical method of parameter determination : in a first step, V, a, r_o are chosen to fit experimental values of R' and of the ratio $\frac{S_0}{S_1}$; in a second step, W, a', r_o' are chosen so as to fit the experimental value of S_0 and to obtain a better agreement for S_1 if necessary ; in these two steps, the spin orbit potential is chosen to have a standard value.

At low energies, the 0^+, 2^+, 4^+ coupling basis was adopted as explained, but at higher energies (10 MeV - 20 MeV), in order to reduce the extensive calculation time, the so-called adiabatic approximation was employed with nearly the same set of optical parameters. The only new adjustement in this energy range has been made for W so as to match the measured [18,19] "elastic" angular distribution (cf Fig.3a). We have chosen to keep W constant above 10 MeV. The experimental [12,20] and calculated neutron total cross sections from 10 MeV to 20 MeV are given in Fig. 3b. The agreement between theoretical and experimental values is quite good. In Fig. 3c a comparison is made in the energy range 2 MeV - 20 MeV between experimental values [14,15,17,19,21] of the total "elastic" cross section and calculated values of the sum of direct elastic and inelastic cross sections (0^+, 2^+, 4^+). It seems to us advisable (as direct and inelastic scattering are not resolved) to compare in the same energy range the experimental non elastic cross section with calculated values of the compound nucleus formation cross section. This comparison is shown in Fig. 3d.

Remark about the Vr_o^n ambiguity

The following example applied to ^{238}U demonstrates clearly that when this procedure of optical parameter determination is employed, the well known Vr_o^n ambiguity disappears. Calculated values of strength functions, potential scattering radius, and total cross sections for different choices of V and r_o are shown in Table 4 along with experimental or recommended values of these data. Results obtained with adopted parameters are in the third column ; in the second and fourth columns results were obtained by varying V and r_o in such a way that the product Vr_o^2 remains constant. In the fifth column r_o was fixed at the value 1.17 fm and V adjusted so as to fit the experimental values of strength functions and potential scattering radius.

IV-2- Statistical model parameters

The discrete levels of ^{238}U introduced in the present calculations are those given in Table 5 from ref. [22]. At low neutron incident energy ($E < 2$ MeV), the continuous level density needed above the energy of the last discrete level (1.1677 MeV) has the following form :

$$\rho_1(E_c) = \frac{1}{T} \exp\left(\frac{E_c - E_0}{T}\right) \qquad (24)$$

where the nuclear temperature T and E_0 are obtained from an adjustment to the discrete level scheme. The resulting values are :

$$E_0 = -0.15 \text{ MeV} \qquad \text{and} \qquad T = 0.41 \text{ MeV}$$

To describe the level density of the compound nucleus ^{239}U, the conventional Fermi-gas formula of Gilbert and Cameron [9] $\rho_2(E_c) \sim \exp\left[2\sqrt{a(E_c - \delta)}\right]$ has been adjusted to the mean level spacing D_{obs} observed at the neutron resonance energies. The chosen value $D_{obs} = 19 \pm 2$ meV [23] gives a corresponding level density parameter $\underline{a} = 30.924$ MeV^{-1} (with a pairing energy $\delta = 0.69$ MeV [Cook 23]).

At higher neutron incident energy ($E > 2$ MeV), the calculations take into account only continuous level densities using the empirical formula of Gilbert and Cameron for all the involved nuclei (^{239}U to ^{236}U) :

$$\begin{aligned} a &= A\,[0.00917\, S_c + 0.120]\ \text{MeV}^{-1} \\ E_x &= 2.5 + 150./A + \delta \end{aligned} \qquad (25)$$

In these expressions, A is the mass number, S_c is the shell correction and E_x is the transition energy below which the level density takes the form (24). In this case the T and E_0 parameters are determined by matching ρ_2 and ρ_1 at the energy E_x .

The fission parameters have been obtained by fitting the calculated total fission cross section to the experimental evaluation recommended by Sowerby [24] . At low incident energies ($E_n < 2$ MeV), the shape of the fission barriers is taken from Weigmann and Theobald [25] . The imaginary part in the second well has been treated in the approximation of complete damping (cf. Appendix).

The characteristics of fission channels ($K^{\pi} = 1/2^-, 1/2^+, 3/2^-, 3/2^+$) have been adjusted following the procedure described above. Resulting values are indicated in Table 6.

In the incident energy range 2 MeV - 20 MeV, the Kl and C parameters (see Appendix) obtained are tabulated in Table 7 together with the other model parameters such as neutron separation energies [26], experimental γ-ray widths [27] and equivalent single fission barrier B_f [28].

V - RESULTS AND DISCUSSION

The coupling scheme and optical parameters were chosen so as to satisfy the carefully chosen experimental constraints, namely the s and p-wave strength functions, the potential scattering radius and the total cross section over the full energy range. The model adjustments emphasize the minima and maxima of the total cross section. This procedure was successful in the determination of a coherent parameter set appropriate to ^{238}U. These same parameters applied to ^{232}Th produced a similar good agreement with the same neutron basic data. Obviously, in this case, different nuclear deformation parameters had to be employed ($\beta_2 = 0.206$, $\beta_4 = 0.086$). Thus, we have confidence in the application of this method to neighbouring nuclei for which no experimental data exist. Though no automatic parameter determination procedure was employed, very good agreement was obtained for the "elastic" angular distribution. We mention for example, in the case of ^{238}U, that the latest "elastic" scattering measurements of Kinney [17] were not yet known when the parameter determination was achieved. Comparisons of these experimental results are shown for incident neutron energies of 6.44 and 8.56 MeV in Fig. 4a and Fig. 4b respectively. At these energies, the experimental resolution was $\leqslant$ 0.309 MeV, and thus not adequate to resolve elastic scattering from inelastic scattering related to the first three excited states. The true shape of differential elastic scattering so differs from that observed at high energies ; for example, comparison is made in Fig. 4c for an incident neutron energy of 14.0 MeV between the observed [31] and the calculated "elastic" scattering angular distributions, whereas Fig. 4d shows at the same energy the calculated elastic and inelastic scattering cross sections.

The theoretical angular distributions of the direct 2^+ and 4^+ component of inelastic scattering at various energies are shown in Fig. 5a and Fig. 5b.

Remark

The new optical model determination procedure employed here was further extended to various spherical (A = 89,93), vibrational (A = 148) or rotational (A = 152,154) nuclei using different coupling schemes. The procedure has also been explained elsewhere (ref. [32]), where it was referred to as the "SPRT" method.

The calculated radiative capture cross section is in good agreement with the experimental data [24] for energies below 1 MeV (Fig. 6). Above this energy the calculated cross sections are very sensitive to the continuous level density parameters E_0 and T (eq. 24). This leads to an overestimation of the radiative capture cross section if compared to the Sowerby experimental evaluation [24] . The comparison between the calculated and experimental total elastic scattering cross sections is very satisfactory as shown in Fig. 7 over the energy range 100 keV - 1 MeV. The compound and direct inelastic scattering cross sections are given up to 2 MeV in Table 8 for the first two excited levels (2^+ at 0.045 MeV and 4^+ at 0.148 MeV). For these two levels, the calculations point out the great importance of the direct excitation process for inelastic scattering mainly above 1 MeV. In the energy range 1 MeV - 3 MeV, these two calculated cross sections seem in fairly good agreement with recent measurements of Smith [29] . For the other excited states the present results are slightly below the experimental and calculated values of MacMurray [22] (Fig. 8).

The (n,2n) and (n,3n) calculated cross sections are tabulated in table 9 . Fig. 9 presents a comparison of these results with experimental measurements [30] . There is good general agreement for the (n,2n) reaction except above 15 MeV where the calculated cross section decreases too rapidly. In this energy range, just above the (n,3n) reaction threshold, the employed spin independent statistical model is certainly not adequate and a more realistic model with angular momentum and parity conservation is necessary. Moreover, to refine the calculations, the preequilibrium emission should be introduced also. Nevertheless, by adjustment to the total fission cross section over a large energy range (2 MeV - 20 MeV), the present method determines the energy variation of widths of several nuclei (^{239}U, ^{238}U and ^{237}U in the case of a ^{238}U target). Using these widths, fission and (n,xn) cross sections of neighbouring nuclei (^{237}U and ^{236}U) can be calculated. In Ref. [6] this method has been extended to U isotopes from ^{232}U to ^{239}U.

CONCLUSION

The coupled channel optical model analysis presented here has been successful in describing a great variety of neutron data for ^{238}U. This success is due to the optical potential determination procedure. The strength and the geometry of the potentials were determined at low neutron energies ($E \leqslant 1$ MeV) by fitting to the strength functions (S_0, S_1), the potential scattering radius (R') and the total cross sections (σ_T (E)). So, for neutron capture calculations it was not necessary to compute adequate neutron transmission coefficients using the so-called "strength function model" or another local optical model parameter set [33] . The energy dependences of the real and imaginary potential strengths were obtained by fitting the total cross section at higher neutron energies. Using this procedure (SPRT-method [32]), it is necessary to adopt an increase of the surface peaked absorption with the neutron energy ; the large experimental uncertainties of neutron non elastic cross sections for ^{238}U did not permit the investigation of the onset of volume absorption. This optical potential determination differs greatly from those usually employed, which are based mainly on fits to the elastic angular distribution. Nevertheless, it is clear that the agreement between our predictions and measurements of "elastic" angular distribution is good. As regards the inelastic neutron scattering cross sections from the members of the ground state rotational band, the present work illustrates clearly the need for coupled channel calculations for deformed nuclei.

It can be seen that the present statistical model analysis shows good general agreement with the various experimental cross sections related to the formation of a compound nucleus. By an adjustment to the total fission cross section, the various neutron, γ-ray and fission branching ratios can be calculated and then used with confidence to determine the cross sections of other reactions such as radiative capture up to 3 MeV, (n,xn) reactions, compound elastic and inelastic scattering. At low incident energy, some characteristics of the two-humped fission barrier are obtained by solving numerically the Schrödinger equation and fitting the results to the total fission cross section. For ^{238}U these channel characteristics are similar to other determinations [40]. At higher incident energy, this method enables both the (n,xn) and fission cross-sections to be properly related.

Thus we have obtained over a large incident energy range a complete and coherent set of a number of important cross sections by using conjointly the optical and statistical models. The methods employed here can be easily extended to provide a consistent set of calculated cross sections for less-known neighbouring nuclei or in energy ranges where experimental data are too scarce.

The authors are gratefully indebted to Dr R.L. WALSH for a critical reading of the manuscript.

APPENDIX

TRANSMISSION COEFFICIENTS AND WIDTHS

γ-ray transmission coefficients

The γ-ray transmission coefficients of equations (11), (17) and (19) are written in the form :

$$T_\gamma(E, J\pi) = 2\pi\, \rho_{J\pi}(E_c)\, \Gamma_\gamma^{J\pi}(E_c) \tag{A1}$$

where $\rho_{J\Pi}(E_c)$ is the Fermi-gas level density [9] of the compound nucleus in its state ($E_c J\Pi$). When the giant dipole resonance is taken into account, the radiative width $\Gamma_\gamma^{J\Pi}(E_c)$ is given by the expression

$$\Gamma_\gamma^{J\pi}(E_c) = C_\gamma \sum_{J'=J-1}^{J'=J+1} \int_0^{E_c} \varepsilon^2 \left[\sigma_1 \frac{(\varepsilon\Gamma_1)^2}{(\varepsilon^2-\varepsilon_1^2)^2+(\varepsilon\Gamma_1)^2} + \sigma_2 \frac{(\varepsilon\Gamma_2)^2}{(\varepsilon^2-\varepsilon_2^2)^2+(\varepsilon\Gamma_2)^2} \right] \frac{\rho_{J'\pi'}(E_c-\epsilon)}{\rho_{J\pi}(E_c)}\, d\epsilon \tag{A2}$$

The proportionality constant C_γ is obtained by normalization to experimental Γ_γ values for slow neutron resonances, when they are known. If not known, Γ_γ values of neighbouring nuclei with the same A parity are taken. σ_1, Γ_1, ε_1 and σ_2, Γ_2, ε_2 are respectively the cross sections, widths and energies of the giant dipole resonance (for ^{238}U cf. [38]). This radiative width can also be deduced from the single particle formalism [4] . Assuming only electric dipole radiations, we have in this case :

$$\Gamma_\gamma^{J\pi}(E_c) = C_\gamma \sum_{J'=J-1}^{J'=J+1} \int_0^{E_c} \epsilon^3\, \rho_{J'\pi'}(E_c-\epsilon) / \rho_{J\pi}(E_c)\, d\epsilon \tag{A3}$$

For lower energies, equation (A3) seems better than equation (A2). The ~~spin-independent radiative width~~ $\Gamma_\gamma(E_c)$ of equations (13), (14), (15), (20) and (21) has the form of equations (A2) and (A3), but without the sum over J' and with a spin-independent level density. When using the simplified statistical model, the single particle formalism is preferred at excitation energies below the neutron separation energy and the giant dipole resonance formalism above this excitation energy.

Neutron transmission coefficients

The neutron penetrabilities $T_{\ell j}(E)$ and compound nucleus formation cross-section $\sigma_c(E)$ needed in the statistical models are deduced from the coupled channel calculations.

The total neutron transmission coefficients (equations (11), (17) and (19) for the exit channels with the target nucleus left in discrete excited states λ (energy E_λ, spin I_λ and parity Π_λ) or in continuous excited states λ' (energies E_m, spin $I_{\lambda'}$, and parity $\Pi_{\lambda'}$) are :

$$T_n(E, J\pi) = \sum_{j'} \sum_{\ell'} \sum_{\lambda} T_{\ell' j'}(E - E_\lambda)\, \delta_{\pi, (-1)^{\ell'} \pi_\lambda} + \frac{1}{2} \sum_{\lambda'} \sum_{j'} \sum_{\ell'} \int_0^{E - E_i} \rho_{I_{\lambda'}}(E - \varepsilon)\, T_{\ell' j'}(\varepsilon)\, d\varepsilon \qquad \text{(A4)}$$

$$= \sum_{\lambda} T_{n(\lambda)}(E - E_\lambda, J\pi)$$

where the angular momentum summations are limited by the usual relations between the total nuclear spin $\vec{J}$, the target spin $\vec{I}_\lambda$ and the spin $\vec{s}$ and orbital momentum $\vec{l}'$ of the neutron :

$$\vec{J} = \vec{I}_\lambda + \vec{j}' \qquad \vec{j}' = \vec{\ell}' + \vec{s} \qquad \text{(A5)}$$

In the r.h.s. of equation (A4), the first term contains a summation over all the λ discrete levels of energy less than E , and the second term takes into account a continuous level density when E is greater than the energy E_1 of the higher discrete level.

The neutron width of the compound nucleus at excitation energy E_c when using the spin-independent statistical model in equations (13), (14), (15), (20) and (21), is given by :

$$\Gamma_n(E_c) = \frac{(2s+1)}{\pi^2 \hbar^2 \rho(E_c)} \mu \int_0^{E_c - S} \epsilon \, \sigma_c(\epsilon)\, \rho(E_c - S - \epsilon)\, d\epsilon \qquad \text{(A6)}$$

In this equation s is the neutron spin, μ the reduced mass in the exit channel, $\rho(E_c)$ and $\rho(E_c-S-\varepsilon)$ are respectively the level densities of the compound and residual nucleus. The formalism of Gilbert and Cameron was chosen for determining the level densities needed in the calculations of these widths. S is the neutron separation energy from the compound nucleus and ε the energy of the emitted neutron.

Fission transmission coefficients

The fission transmission coefficients $T_f(E,JK\Pi)$ in equations (11), (17) and (19) are computed exactly for a fission barrier defined in terms of two parabolic peaks connected by a third parabola for the second well (Fig. 1).

Let us denote by V and W the real and imaginary parts of the potential. At the excitation energy E_c these regions are characterized as follows :

Region III : $\beta \geq \beta_e$, $V = 0$, $W = 0$.

Relative to the β deformation coordinates in the considered fission channel, the plane wave function is given by :

$$\Psi_{JK\pi} = \exp(-ik\beta) - \eta_{JK\pi} \exp(ik\beta) \qquad \text{(A7)}$$

where $k = \sqrt{2\mu E_c}/\hbar$ and μ is the assumed constant inertial parameter.

Region I : $\beta \leqslant \beta_i$ $V = 0$ $W \neq 0$

The wave function for complete damping is :

$$\psi_{JK\pi} = A_{JK\pi} \exp\left(-i k\beta\right) \tag{A8}$$

and the flux Φ_d completely absorbed :

$$\Phi_d\left(JK\pi\right) = \left|A_{JK\pi}\right|^2 \tag{A9}$$

Region II : $\beta_i \leqslant \beta \leqslant \beta_e$

In this region, the potential is

$$V_j = E_j + (-)^j \cdot \frac{1}{2}\mu\ \omega_j^2\ \left(\beta - \beta_j\right)^2 \qquad (j = 1, 2, 3,) \tag{A10}$$

with $E_1 \equiv E_A$, $E_2 \equiv E_{II}$, $E_3 \equiv E_B$. ω_j is the barrier width. The negative parabolic imaginary potential is localized in this region with a maximum absolute value W_m at $\beta = \beta_2$. W_m can be determined from photofission anisotropies. If E_γ is the γ-ray incident energy, the following linear dependence has been found to be adequate [5].

$$W_m\ (MeV) = W_o\left(E_\gamma - E_2 - 2\ \right) + W_I \qquad (E \text{ in MeV}) \tag{A11}$$

The absorbed flux in this well is :

$$\Phi_a\left(JK\pi\right) = 1 - \left|A_{JK\pi}\right|^2 - \left|\eta_{JK\pi}\right|^2 \tag{A12}$$

The requirement that the wave functions and their derivatives be continuous at the points β_i and β_e determines the coefficients $A_{JK\pi}$ and

$n_{JK\Pi}$. In region II the wave function is calculated by solving the Schrödinger equation :

$$\left[-\frac{\hbar^2}{2\mu}\frac{d^2}{d\beta^2}+V(\beta)-i\,W_{II}(\beta)-E^*\right]_{JK\pi}\psi_{JK\pi}(\beta)=0 \qquad \text{(A13)}$$

At excitation energies close to E_B we can assume

$$T_f(E,JK\Pi)=\left[\Phi_d(JK\pi)+\Phi_a(JK\pi)\,\frac{P_A(JK\pi)}{P_A(JK\pi)+P_B(JK\pi)}\right]N_f(JK\pi) \qquad \text{(A14)}$$

where $P_A(JK\Pi)$ and $P_B(JK\Pi)$ are the Hill-Wheeler [39] penetration factors for the single barriers A and B . N_f (JKΠ) is the effective number of fission channels taking into account the effect of other (J,K,Π) channels higher in energy.

At excitation energy $E_c \sim E_A$, the transmission coefficient becomes :

$$T_f(E,JK\Pi)=\left[\Phi_d(JK\pi)+\Phi_a(JK\pi)\,P_A(JK\pi)\right]N_f(JK\pi) \qquad \text{(A15)}$$

The transition from equation (A14) to equation (A15) is done at the excitation energy where $P_A(JK\Pi) + P_B(JK\Pi) = 1$.

In the spin independent statistical calculations (E_n > 2 MeV) we consider an equivalent single parabolic fission barrier.

At excitation energies E^* high enough above the height B_f of this barrier, the fission width is

$$\Gamma_f(E)=\frac{K_1}{2\pi\rho(E^*)}\int_0^{E^*-B_f}\rho^f(\varepsilon)\,d\varepsilon \qquad \text{(A16)}$$

where K_1 is an adjustable parameter. ρ^f (ε) is the Fermi-gas level density at energy ε for the saddle point deformation where the level density parameter is $\underline{a}_f$ instead of $\underline{a}$. It has been found convenient to choose a simple energy dependence of a_f in the form :

$$a_f = a + \frac{C}{E^*} \tag{A17}$$

where C is adjustable.

In this energy range, the different couples of free parameters K_1 and C of the involved nuclei are deduced by fitting to the experimental total fission cross-sections.

At excitation energies close to the fission barrier B_f , the fission width is determined from the Hill-Wheeler [39] penetrability factor

$$\Gamma_f(E^*) = \frac{K_1}{2\pi\varrho(E^*)} \int_0^{E^*} \frac{\varrho^f(\varepsilon)\, d\varepsilon}{1 + \exp[-2\pi(E^* - B_f - \varepsilon)/\hbar\omega]} \tag{A18}$$

where ω is the circular frequency of the inverted harmonic oscillator potential which simulates the fission barrier.

REFERENCES

[1] T. TAMURA, Rev. Mod. Phys. 37 (1965) 679.
T. TAMURA, Oak Ridge National Laboratory Report ORNL-4152 (1962).

[2] W. HAUSER, H. FESHBACH, Phys. Rev. 87 (1952) 366.

[3] P.A. MOLDAUER, Rev. Mod. Phys. 36 (1964) 1074.
Phys. Rev. 135B (1964) 642.
Phys. Rev. 171 (1968) 1164.

[4] J.M. BLATT, V.F. WEISSKOPF, Theoretical Nuclear Physics, Ed. Wiley (1952)

[5] P. THOMET, Commissariat à l'Energie Atomique Report CEA-R-4631 (1974).

[6] J. JARY, Commissariat à l'Energie Atomique Report CEA-R-4647 (1975).

[7] Ch. LAGRANGE, To be published.

[8] C.A. UTTLEY, Comptes Rendus du Congrès International de Physique Nucléaire, Paris (juillet 1964), Ed. CNRS (Vol. II, p. 700).

[9] A. GILBERT, A.G.W. CAMERON, Can. J. Phys. 43 (1965) 1446.

[10] P. MÖLLER, Nucl. Phys. A192 (1972) 529.

[11] A. ADAM, J. CABE, M. LABAT, M. LAURAT, M. LONGUEVE, Centre d'Etudes de Bruyères-le-Châtel, Internal Report unpublished, (1969).

[12] S.H. HAYES, P. STOLER, J.M. CLEMENT, C.A. GOULDIN, Nucl. Sc. Eng. 50 (1973) 243.

[13] A. SMITH et al., Argonne National Laboratory Memorandum, Comments on Inelastic Neutron Scattering from ^{238}U (1973).

[14] R. BATCHELOR, W.B. GILBOY, J.M. TOWLE, Nucl. Phys. 65 (1965) 236.

[15] M. WALT, J.R. BEYSTER, Los Alamos National Laboratory Report LA-2061 (1956).

[16] M.M. KNITTER, M. COPPOLA, N. AHMED, B. JAY, Zeit. für Phys. 244 (1971) 358.

[17] W.E. KINNEY, F.G. PEREY, Oak Ridge National Laboratory Report ORNL-4804 (1973).

[18] B.Y. GUZHOVSKII, At. Energ. 11 (1961) 395.
Sov. J. At. Energ. 11 (1962) 1041.

[19] C.L. HUDSON, W. SCOTT WALKER, S. BERKO, Phys. Rev. 128 (1962) 1271.

[20] P.H. BOWEN, J.P. SCANLON, G.H. STAFFORD, J.J. TRESHER, P.E. HODGSON, Nucl. Phys. 22 (1961) 640.

[21] L. CRANBERG, J.S. LEVIN, Phys. Rev. 109 (1958) 2063.

[22] W.R. McMURRAY, Annual Research Report (1973) SUNI 28.

[23] F. POORTMANS et al., NEANDC(E) 163 U (1974) 149.
M.G. SOWERBY, NEANDC (E) 163 U (1974) 183.
H. MALECKY, L.B. PIKEL'NER, I.M. SLAMATIN, E.I. SHARAPOV, Sov. J.Nucl. Phys. 13 (1971) 133.
J.L. COOK, H. FERGUSON, A.R. DEL MUSGROVE, Aust. J. Phys. 20 (1967) 477.
H. BABA, Nucl. Phys., A159 (1970) 625.

[24] M.G. SOWERBY, B.H. PATRICK, D.S. MATHER, Annals of Nucl. Sc. and Eng. 1 (1974) 409. - AERE-R-7273 (1973).
W.P. POENITZ, Préprint (ANL).

[25] H. WEIGMANN, J.P. THEOBALT, Nucl. Phys. A187 (1972) 305.

[26] A. H. WAPSTRA, N.B. GOVE, Nucl. Data Tables 9 (1971) n° 4-5.

[27] P.E. VOROTNIKOV, Sov. J. Nucl. Phys. 5 (1967) 728.

[28] V.E. VIOLA, B.D. WILKINS, Nucl. Phys. 82 (1966) 65.
G.I. BELL, Phys. Rev. 158 (1967) 1127.

[29] P. GUENTHER, A. SMITH, Inelastic Neutron Excitation of the Ground State Rotational Band of ^{238}U. Washington Conf. (3-7 mars 1975).

[30] J.D. KNIGH, R.V. SMITH, B. WARREN, Phys. Rev. 112 (1958) 259.
J.L. PERKIN, R.F. COLEMAN, J. Nucl. Energ. 14 (1961) 69.
D.S. MATHER, P.F. BAMPTON, R.E. COLES, G. JAMES, P.J. NIND, AWRE 072/72 (1972).
J.H. LANDRUM, R.J. NAGLE, M. LINDNER, Phys. Rev. C8 (1973) 1938.
J. FREHAUT, G. MOSINSKI, CEA Report CEA-4627 (1974).
A. ACKERMANN, M. BORMANN, W. SOOBEL, NEANDC(E) 161 U (1974).

[31] J. VOIGNIER, Commissariat à l'Energie Atomique Report, CEA-R-3503 (1968).
G. MOUILHAYRAT, Centre d'Etudes de Bruyères le Châtel Private Communication (1969).
J.L. KAMMERDIENER, UCRL 51232 (1972).

[32] J.P. DELAROCHE, Ch. LAGRANGE, J. SALVY, Review Paper n° 5, IAEA Consultants Meeting on "the Use of Nuclear Theory in Neutron Nuclear Data Evaluation" ICTP, Trieste (8-12 december 1975).

[33] P. RIBON, E. FORT, J. KREBS, TRAN QUOC THONG, note CEA-N-1832 (1975)

[34] J.J. SCHMIDT, Neutron Cross Sections for Fast Reactors Materials, KFK Report KFK (120) (EANDC-E-35-V) (1966).

[35] A.B. SMITH, Nucl. Phys. 47 (1963) 633.

[36] R.C. ALLEN, R.B. WALTON, R.B. PERKINS, R. OLSON, R.F. TASCHEK, Phys. Rev. 104 (1956) 731.

[37] E. BARNARD, A. FERGUSON, W.R. McMURRAY, I.J. VAN HEERDEN, Nucl. Phys. 80 (1966) 46.

[38] A. VEYSSIERE, H. BEIL, R. BERGERE, P. CARLOS, A. LEPÊTRE, N.P.A. 199 (1973) 45.

[39] D.L. HILL, J.A. WHEELER, Phys. Rev. 89 (1953) 1102.

[40] B.B. BACK, O. HANSEN, H.C. BRITT, J.D. GARRETT, Phys. Rev. C9 (1974) 1924.
J.E. LYNN, Report AERE-R-7468 (1974).

Base states	V MeV	r_0 fermis	a fermis	W MeV	r_0' fermis	a' fermis	V_s MeV
$(0^+, 2^+)$	47.4 - 0.3 E	1.25	0.65	3 + 0.3E $E \leq 4$ MeV 3.72+0.12E $E \geq 4$MeV	1.250	0.70	7.50
$(0^+, 2^+, 4^+)$	47.5 - 0.3 E	1.24	0.62	2.7+0.4E $E \leq 10$MeV 6.7 $E \geq 10$ MeV	1.260	0.580	7.50

TABLE 1

Optical potential parameters for each set of base states

TABLE 2

	$S_0 \times 10^4$	$S_1 \times 10^4$	R'(fermis)
Experimental	1.00 ± 0.15	2.5 ± 0.5	9.18 ± 0.18
Theoretical (0^+, 2^+)	0.94	1.96	9.08
Theoretical (0^+, 2^+, 4^+)	0.95	2.14	9.24

Comparison between experimental and theoretical values of s and p-wave strength functions (S_0, S_1) and potential scattering radius (R') for ^{238}U. The experimental values are taken from reference [8] . The optical model parameters are those of table 1.

Coupling basis $0^+, 2^+, 4^+$	Optical parameter set of table 1	V = 47.0 modified parameter	V = 48.0 modified parameter	W = 3.33 a' = 0.47 modified parameters	V_s = 0 modified parameter
$S_0 \times 10^4$	0.95	1.06	0.89	0.99	0.92
$S_1 \times 10^4$	2.14	1.89	2.57	2.01	2.17
R'(fermis)	9.24	9.45	9.02	9.20	9.24

TABLE 3

Sensitivity of calculated values of strength functions and scattering radius to various optical potential parameters.

	Experimental or recommended values (1)	r_o = 1.31 fm V = 42.56 MeV Vr_o^2 adjustment (2)	r_o = 1.240 Fm V = 47.5 MeV adopted parameters (3)	r_o = 1.17 Fm V = 53.35 MeV Vr_o^2 adjustment (4)	r_o = 1.17 Fm V = 52.0 MeV adjustment to S_0, S_1, R' (5)
$S_0 \times 10^4$	1.00 ± 0.15	1.04	0.95	0.85	1.05
$S_1 \times 10^4$	2.5 ± 0.5	1.67	2.14	2.78	2.07
R'(fermis)	9.18 ± 0.18	9.80	9.24	8.71	9.23
σ_T (10keV) barns		17.02	15.41	13.90	15.70
σ_T (100keV) barns	12.21	12.74	12.02	11.39	11.73
σ_T (500keV) barns	8.62	8.57	8.52	8.51	8.00
σ_T (1 MeV) barns	7.18	7.34	7.14	7.05	6.48

TABLE 4

Vr_o^n ambiguities for ^{238}U

Experimental values for S_0, S_1 and R' are taken from [8] and recommended values of the total cross sections (σ_T) from ENDF/BIV.

Energy (MeV)	Spin	Parity
0.	0.	+
0.045	2	+
0.148	4	+
0.307	6	+
0.6801	1	-
0.7319	3	-
0.8266	5	-
0.9272	0	+
0.9309	1	-
0.9503	2	-
0.9663	2	+
0.9974	[illegible]	+
0.9974	3	-
1.0373	2	+
1.0459	4	-
1.06	2	+
1.06	4	+
1.1056	3	+
1.1285	4	+
1.1285	2	-
1.1677	3	-
1.1677	4	+

TABLE 5

Energy level scheme of ^{238}U taken from reference [22].

Fission channel	E_A	ω_A	E_{II}	ω_{II}	E_B	ω_B			$N_f^{K\pi}$
$K\pi$							1 MeV	1,2 MeV	1,6 MeV
1/2 (-)	6.3947	1,05	2.4847	1	6.0747	0.5	0.348	0.516	2.737
1/2 +	6.4117	"	2.507	"	6.097	"	1.120	1.239	2.465
3/2 -	6.357	"	2.447	"	6.037	"	0.411	0.673	2.662
3/2 +	6.3919	"	2.4819	"	6.0719	"	1.29	1.421	2.368
$\sum_{K\pi} N_f^{K\pi}$							3.169	3.849	10.232

TABLE 6

Adjusted values of some fission parameters (see Fig. 1). The first column gives the fission channels considered in the present calculations. Columns 2 to 7 give the adopted values, in MeV, of their heights and curvature characteristics. The last three columns give the effective numbers of fission channels and their sum at the incident neutron energies indicated in MeV.

U isotopes	S_n(MeV)	B_f(MeV)	Γ_γ^{exp}(eV)	K_1	C
239	4.8032	6.15	0.024	2.308	0.45
238	6.1436	5.80	0.035	0.602	0.00
237	5.1245	6.30	0.029	5.00	0.95
236	6.5451	5.75	0.035	1.374	0.00

TABLE 7

Neutron separation energies, fission barriers, experimental γ-ray widths and adjusted parameters of the (n,xnf) and (n,xn) cross sections.

TABLE 8

E (MeV)	45.0 keV (2+)		148.0 keV (4+)	
	CN	DI	CN	DI
0.060	0.1685	0.0018		
0.070	0.2656	0.0036		
0.080	0.3465	0.0059		
0.090	0.4151	0.0085		
0.100	0.4743	0.0113		
0.200	0.8139	0.0453	0.0051	0.0001
0.300	0.9704	0.0793	0.0292	0.0014
0.400	1.0512	0.1109	0.0699	0.0052
0.500	1.0963	0.1416	0.1219	0.0122
0.600	1.1234	0.1720	0.1834	0.0225
0.700	1.1122	0.2024	0.2460	0.0356
0.800	1.0405	0.2322	0.2853	0.0507
0.900	0.9882	0.2611	0.3264	0.0669
1.000	0.8765	0.2883	0.3478	0.0833
1.200	0.5753	0.3360	0.2860	0.1140
1.400	0.4073	0.3720	0.2320	0.1390
1.600	0.2987	0.3980	0.1929	0.1580
2.000	0.1868	0.4240	0.1383	0.1800

Compound (CN) and direct (DI) inelastic scattering cross sections for the first two excited states in ^{238}U. Cross sections are given in barn.

Neutron Incident Energy (MeV)	(n,2n) cross-section (Barn)	(n,3n) cross-section (Barn)	(n,f) cross-section (Barn)	(n,n'f) cross-section (Barn)	(n,2nf) cross-section (Barn)	(n,3nf) cross-section (Barn)	Total fission cross-section
2			0.521				0,521
3			0.519				0,519
4			0,508				0,508
5			0.522	$0.25\ 10^{-5}$			0,522
5,5			0.533	$0{,}24\ 10^{-3}$			0,533
6			0.541	0.019			0,560
6,5	0.038		0,548	0,214			0,763
7	0.363		0,554	0.363			0,917
8	1.108		0,558	0,410			0,968
9	1.47		0.609	0,376			0.985
10	1.63		0,619	0,394			1,013
11	1.70		0.611	0.414	$0.38\ 10^{-10}$		1.025
11,5	1.72	$0.36\ 10^{-3}$	0,607	0,419	$0.68\ 10^{-9}$		1,026
12	1.72	0.032	0.603	0.416	$0.45\ 10^{-7}$		1,019
13	1.35	0.43	0.597	0,408	$0.99\ 10^{-5}$		1.007
14	0.78	0.90	0.591	0.416	0.088		1.095
15	0.39	1.13	0,585	0,40	0.26		1.245
16	0.20	1.23	0.580	0.39	0.35		1,32
17	0.112	1.29	0.576	0.37	0.39	$0.43\ 10^{-6}$	1.336
18	0.065	1.32	0.572	0,36	0.41	$0.90\ 10^{-3}$	1.342
19	0.039	1.28	0.567	0.35	0.39	0.076	1.383
20	0.024	1.11	0.562	0,34	0.38	0.25	1,532

TABLE 9

(n,xn) and (n,xnf) cross sections of ^{238}U in the energy range 2 MeV - 20 MeV calculated from the statistical model.

FIGURE CAPTIONS

Fig. 1

a) Real part $V(\beta)$ and imaginary part $W(\beta)$ of the double-humped fission barrier.

b) Adopted shape of the fission barrier for the penetrability calculations.

Fig. 2

Choice of the coupling basis

The curves are coupled channel calculations using two sets of base states. The optical model parameters are the ones of table 1.

- Total neutron cross section

  a) $0.01\ \text{MeV} \leqslant E \leqslant 1\ \text{MeV}$
  b) $1\ \text{MeV} \leqslant E \leqslant 10\ \text{MeV}$

- "Elastic" differential scattering neutron cross section for an incident energy of :

  c) 4 MeV
  d) 7.54 MeV

Fig. 3

Comparisons of experimental and calculated values of neutron cross sections in the energy range 10 - 20 MeV. The curves are coupled channel calculations using adiabatic approximation.

a) "Elastic" differential scattering neutron cross section for an incident energy of 15 MeV.
b) Total neutron cross section.
c) Integrated "elastic" neutron cross section.
d) Comparison of calculated compound nucleus formation cross section to experimental values of non elastic neutron cross section extracted from the compilation made by SCHMIDT [34].

Fig. 4

"Elastic" differential scattering neutron cross sections as tests of the adopted parameterization for an incident energy of

a) 6.44 MeV

b) 8.56 MeV

c) 14 MeV

d) the various components of the differential "elastic" scattering neutron cross section for an incident energy of 14 MeV

Fig. 5

Calculated values of the direct inelastic differential scattering neutron cross section to the levels

a) 2^+ (45 keV)

b) 4^+ (148 keV)

Fig. 6

Calculated neutron radiative capture of ^{238}U from 1 keV to 2 MeV. The experimental data are the ones of Ref. [24].

Fig. 7

Comparisons of experimental and calculated values of the elastic scattering cross section. The experimental values are from references [35,36,37].

Fig. 8

Calculated neutron inelastic cross sections of the excited discrete levels of ^{238}U. The direct inelastic cross section is included for the first two levels. The experimental data are the ones of references [22] and [29]. For the first two levels, the dashed curve gives the ENDF-BIV evaluation; for the other levels, the dashed curve represents the results of calculations from reference [22].

Fig.9

a) Calculated neutron fission cross section of ^{238}U (full line) adjusted to the experimental evaluation of Sowerby (Ref.[24]) (dashed curve).

b) calculated (n,2n) and (n,3n) cross sections compared to experimental data of references [30].

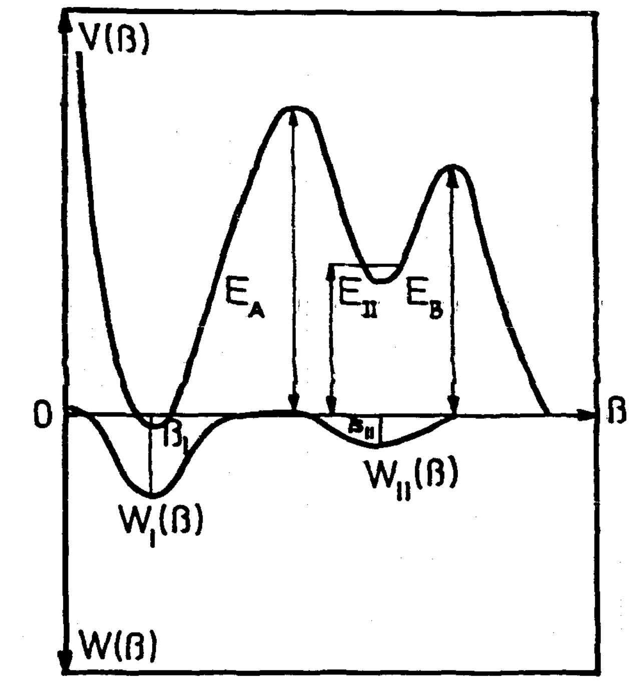
V(ß)
E_A
E_II
E_B
0
ß
ß_I
ß_II
W_I(ß)
W_II(ß)
W(ß)

(a)

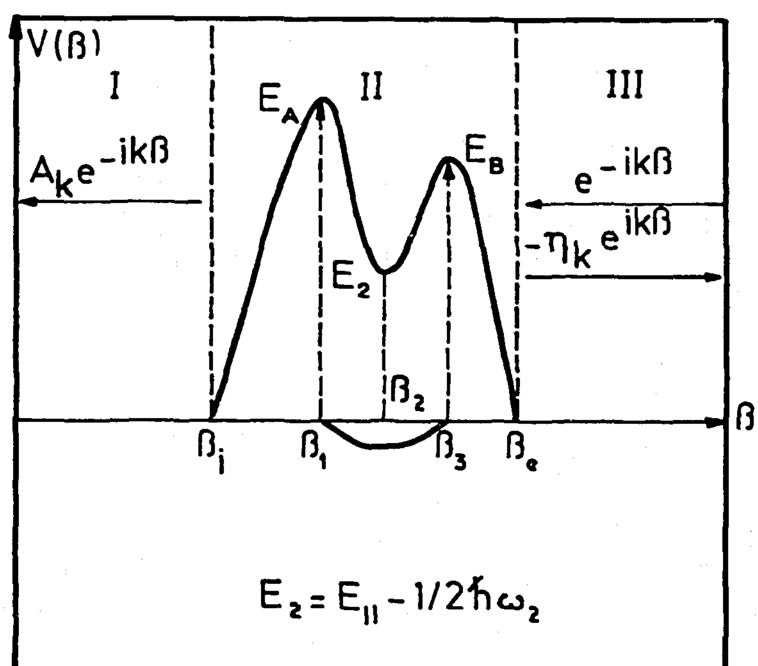
V(ß)
I
II
III
E_A
E_B
A_k e^{-ikß}
e^{-ikß}
-η_k e^{ikß}
E_2
ß_2
ß
ß_i
ß_1
ß_3
ß_e
E_2 = E_II - 1/2 ħω_2

(b)

Fig. 1

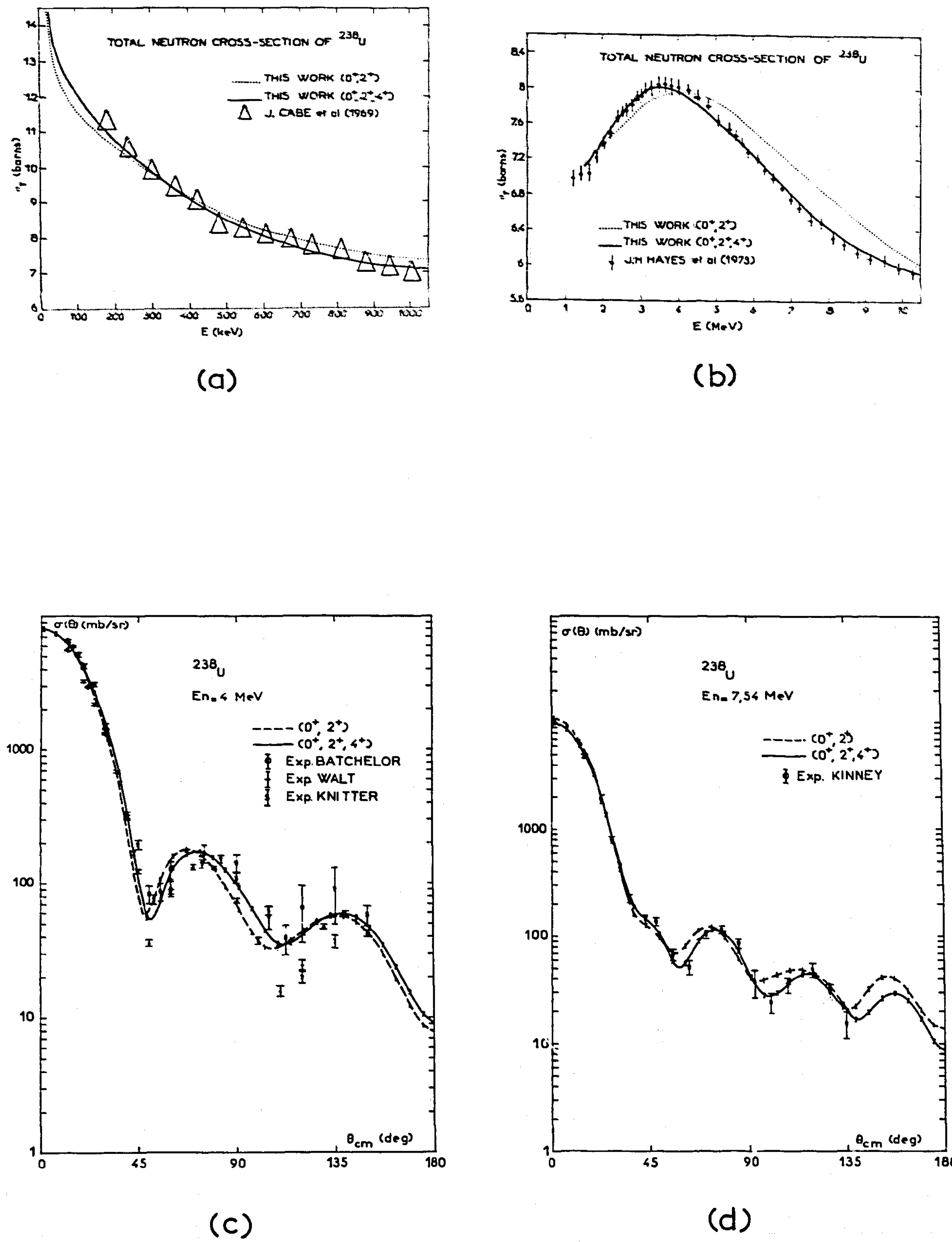

TOTAL NEUTRON CROSS-SECTION OF ²³⁸U
THIS WORK (0⁺,2⁺)
THIS WORK (0⁺,2⁺,4⁺)
J. CABE et al (1969)
(barns)
E (keV)
(a)
TOTAL NEUTRON CROSS-SECTION OF ²³⁸U
THIS WORK (0⁺,2⁺)
THIS WORK (0⁺,2⁺,4⁺)
J.H HAYES et al (1973)
(barns)
E (MeV)
(b)
σ(θ) (mb/sr)
238U
En= 4 MeV
(0⁺, 2⁺)
(0⁺, 2⁺, 4⁺)
Exp. BATCHELOR
Exp. WALT
Exp. KNITTER
θcm (deg)
(c)
σ(θ) (mb/sr)
238U
En= 7,54 MeV
(0⁺, 2⁺)
(0⁺, 2⁺, 4⁺)
Exp. KINNEY
θcm (deg)
(d)

Fig. 2

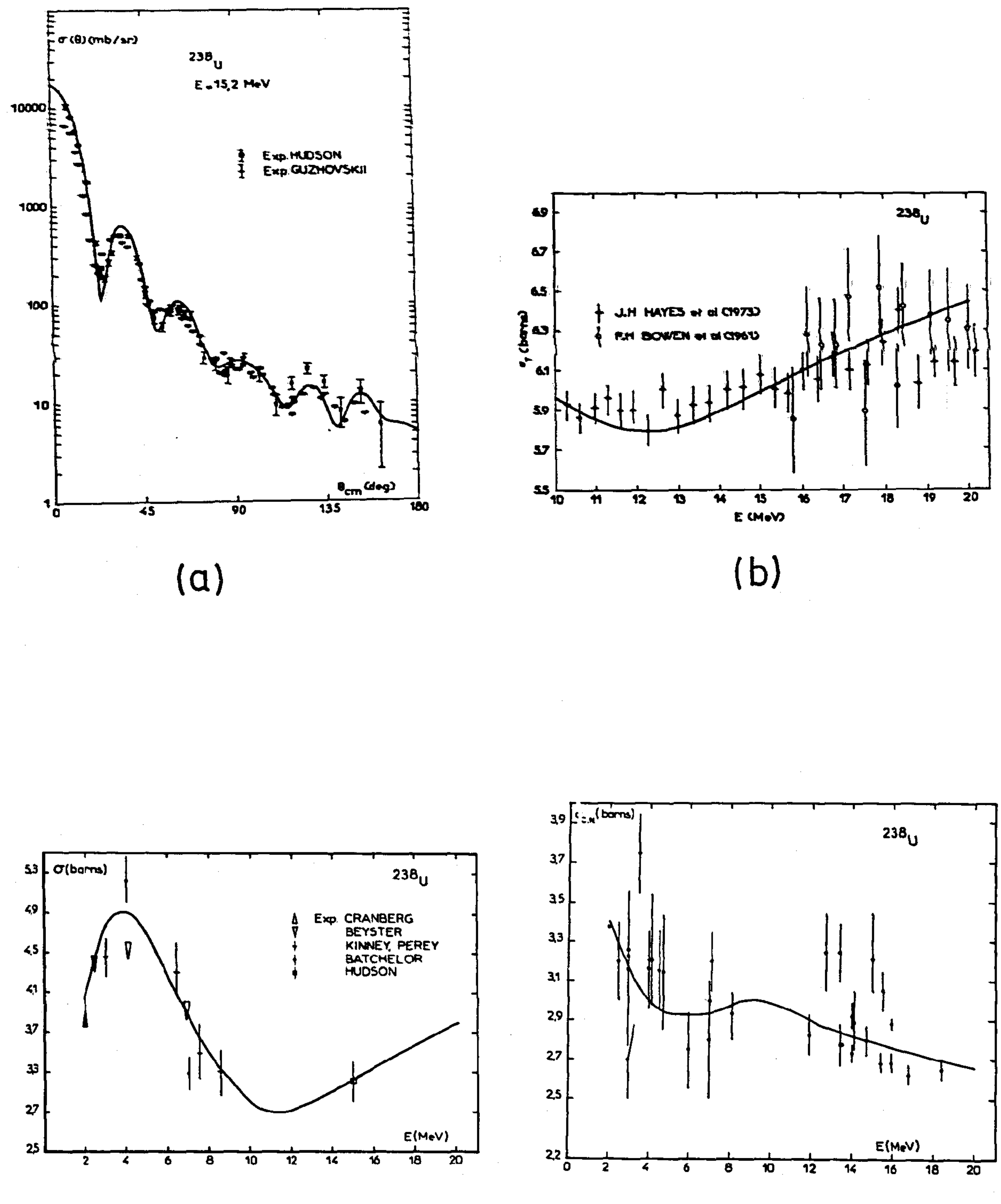

σ(θ) (mb/sr)
238U
E = 15,2 MeV
Exp. HUDSON
Exp. GUZHOVSKII
θcm (deg)
(a)
238U
J.H HAYES et al (1973)
P.H BOWEN et al (1961)
σT (barns)
E (MeV)
(b)
σ(barns)
238U
Exp. CRANBERG
BEYSTER
KINNEY, PEREY
BATCHELOR
HUDSON
E(MeV)
(c)
238U
E(MeV)
(d)

Fig. 3

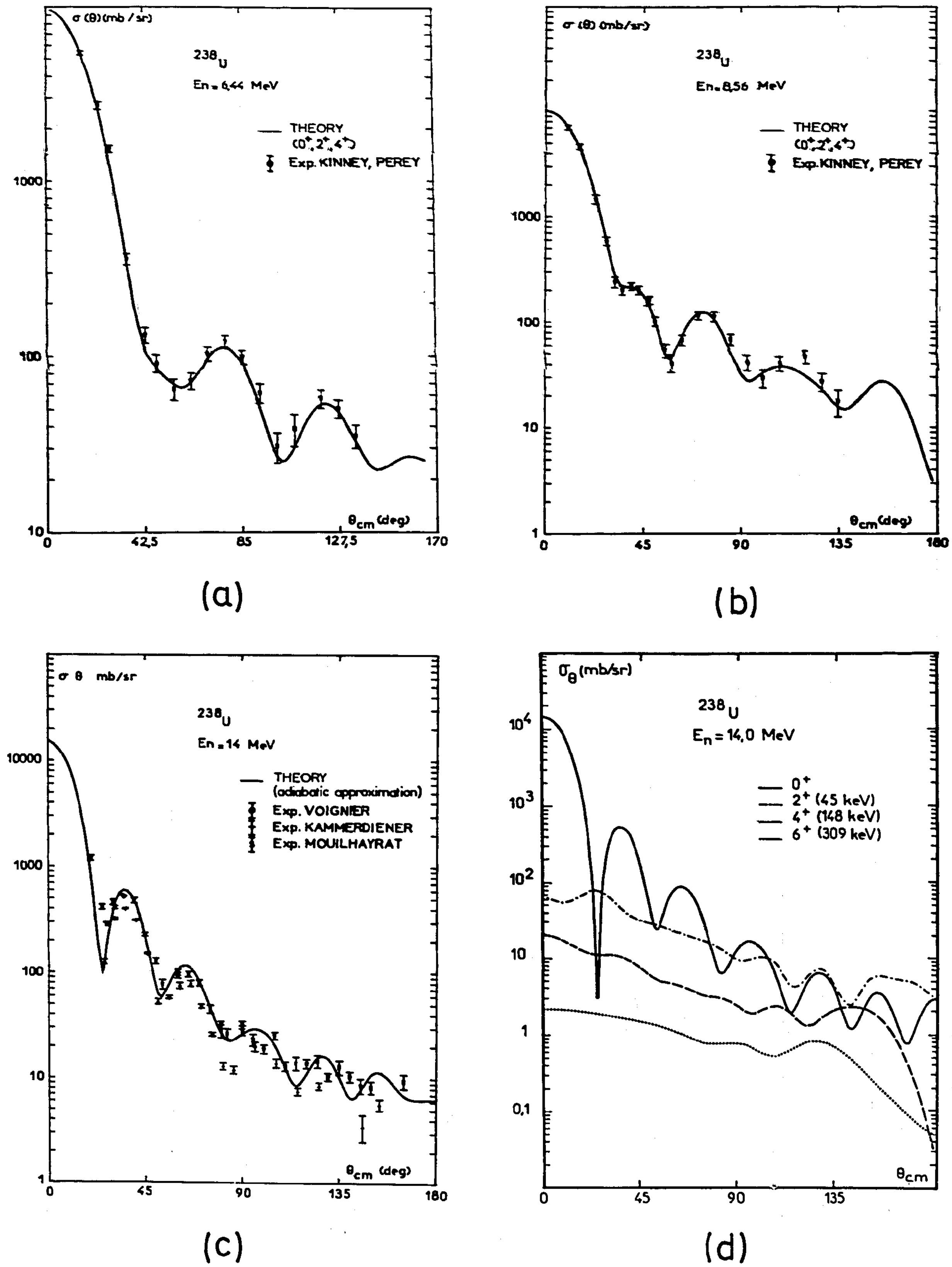
σ (θ) (mb / sr)
238U
En = 6,44 MeV
THEORY
(0+, 2+, 4+)
Exp. KINNEY, PEREY
θcm (deg)
10
100
1000
0
42,5
85
127,5
170
(a)
σ (θ) (mb/sr)
238U
En = 8,56 MeV
THEORY
(0+, 2+, 4+)
Exp. KINNEY, PEREY
θcm (deg)
1
10
100
1000
0
45
90
135
180
(b)
σ θ mb/sr
238U
En = 14 MeV
THEORY
(adiabatic approximation)
Exp. VOIGNIER
Exp. KAMMERDIENER
Exp. MOUILHAYRAT
θcm (deg)
1
10
100
1000
10000
0
45
90
135
180
(c)
σθ (mb/sr)
238U
En = 14,0 MeV
0+
2+ (45 keV)
4+ (148 keV)
6+ (309 keV)
θcm
0,1
1
10
10²
10³
10⁴
0
45
90
135
(d)

Fig. 4

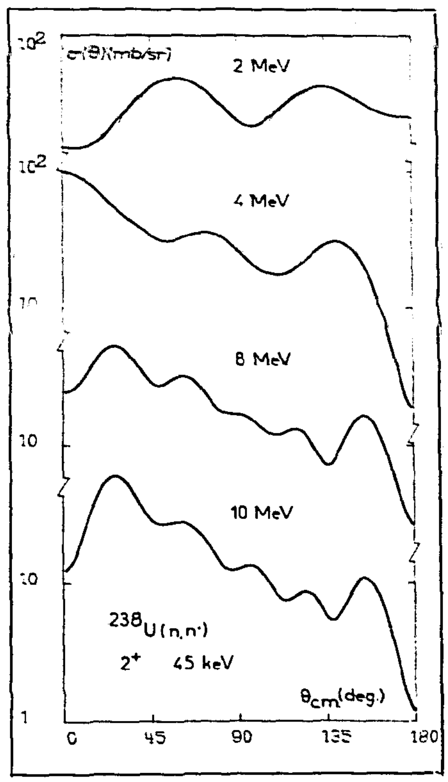

σ(θ)(mb/sr)
2 MeV
4 MeV
8 MeV
10 MeV
^{238}U(n,n')
2+ 45 keV
θcm(deg.)
0
45
90
135
180

(a)

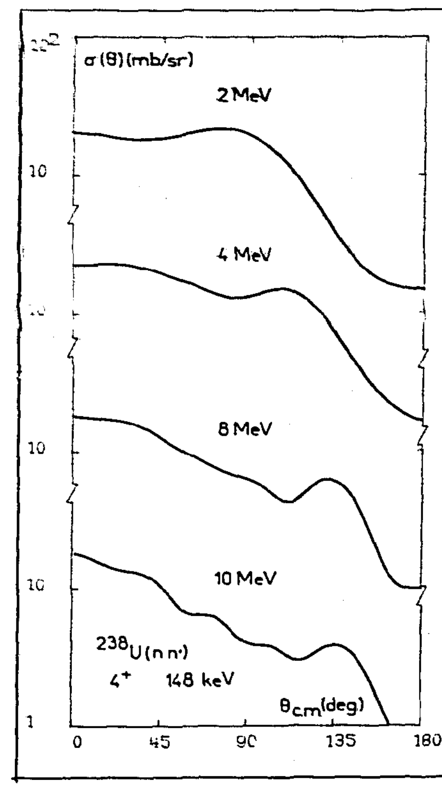

σ(θ)(mb/sr)
2 MeV
4 MeV
8 MeV
10 MeV
^{238}U(n,n')
4+ 148 keV
θcm(deg)
0
45
90
135
180

(b)

Fig. 5

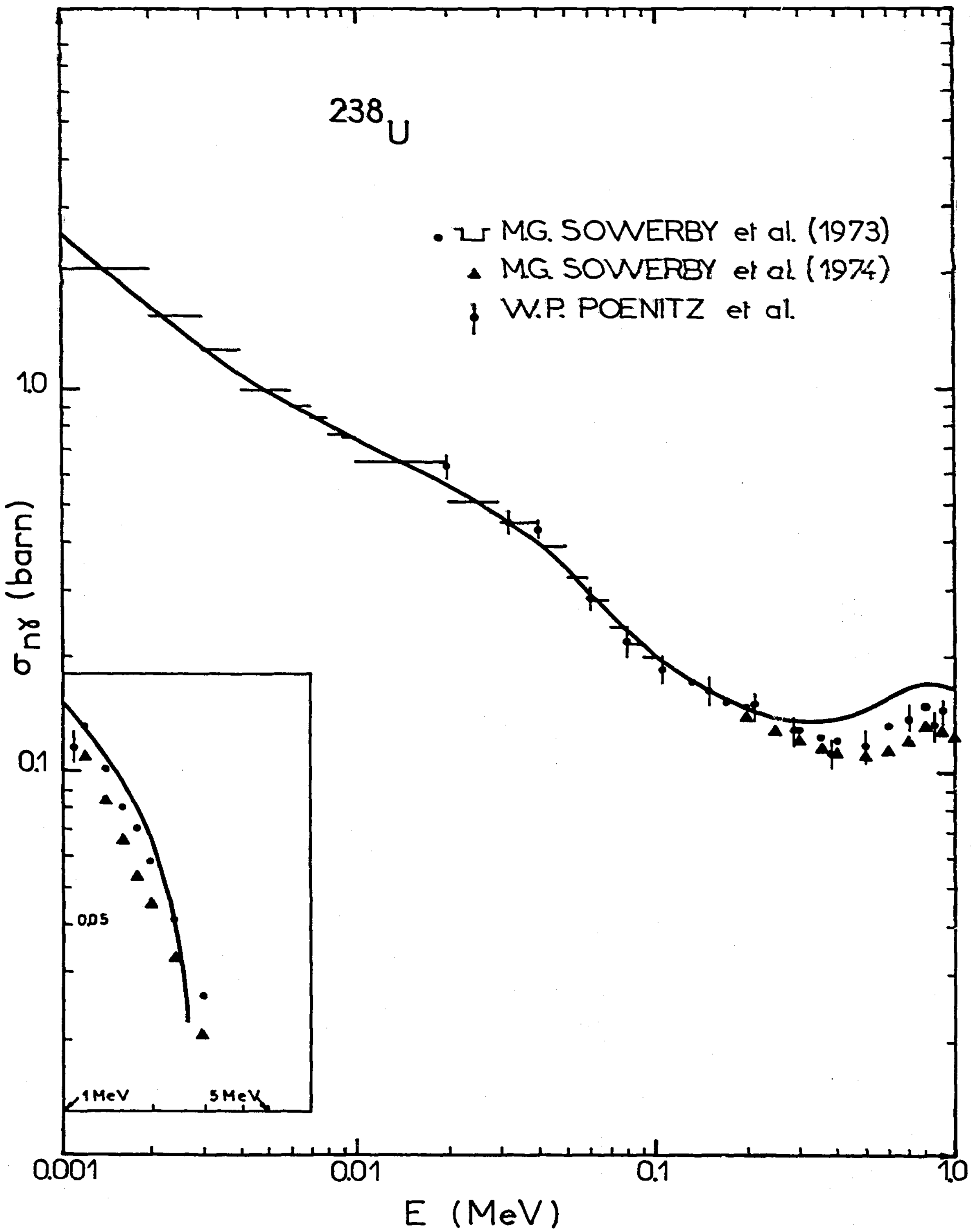
238U
M.G. SOWERBY et al. (1973)
M.G. SOWERBY et al. (1974)
W.P. POENITZ et al.
1.0
0.1
σnγ (barn)
0.05
1MeV
5MeV
0.001
0.01
0.1
1.0
E (MeV)

Fig. 6

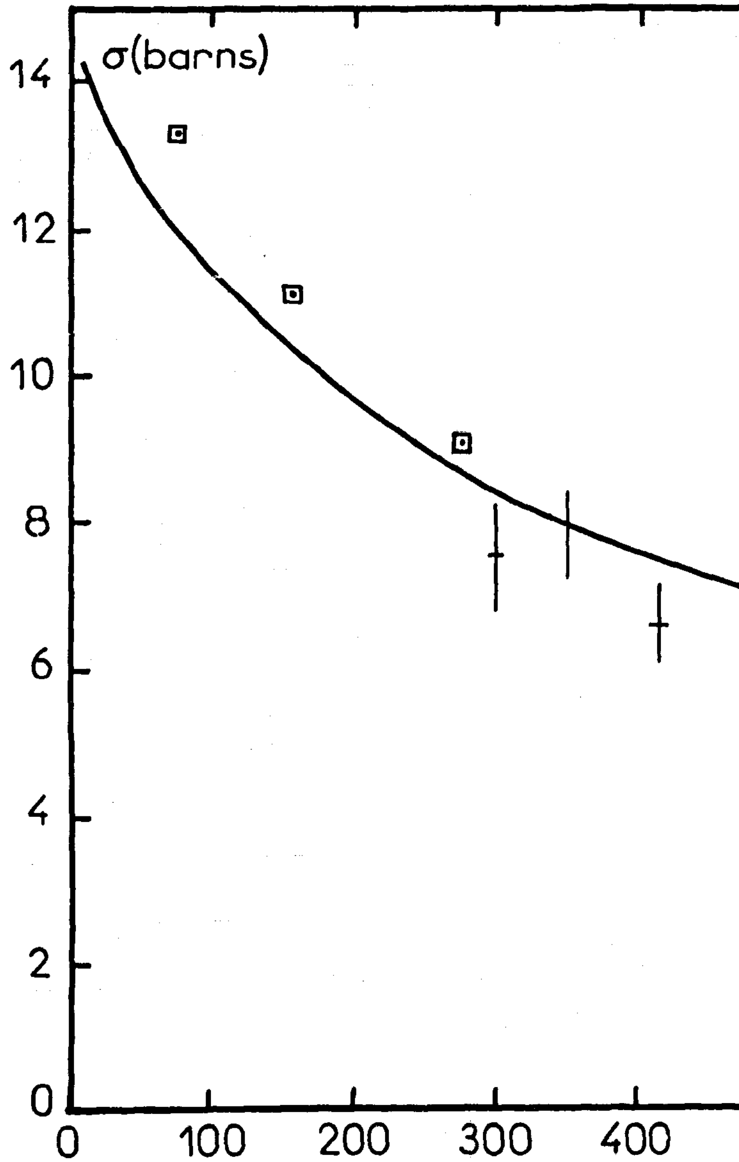

Fig. 7

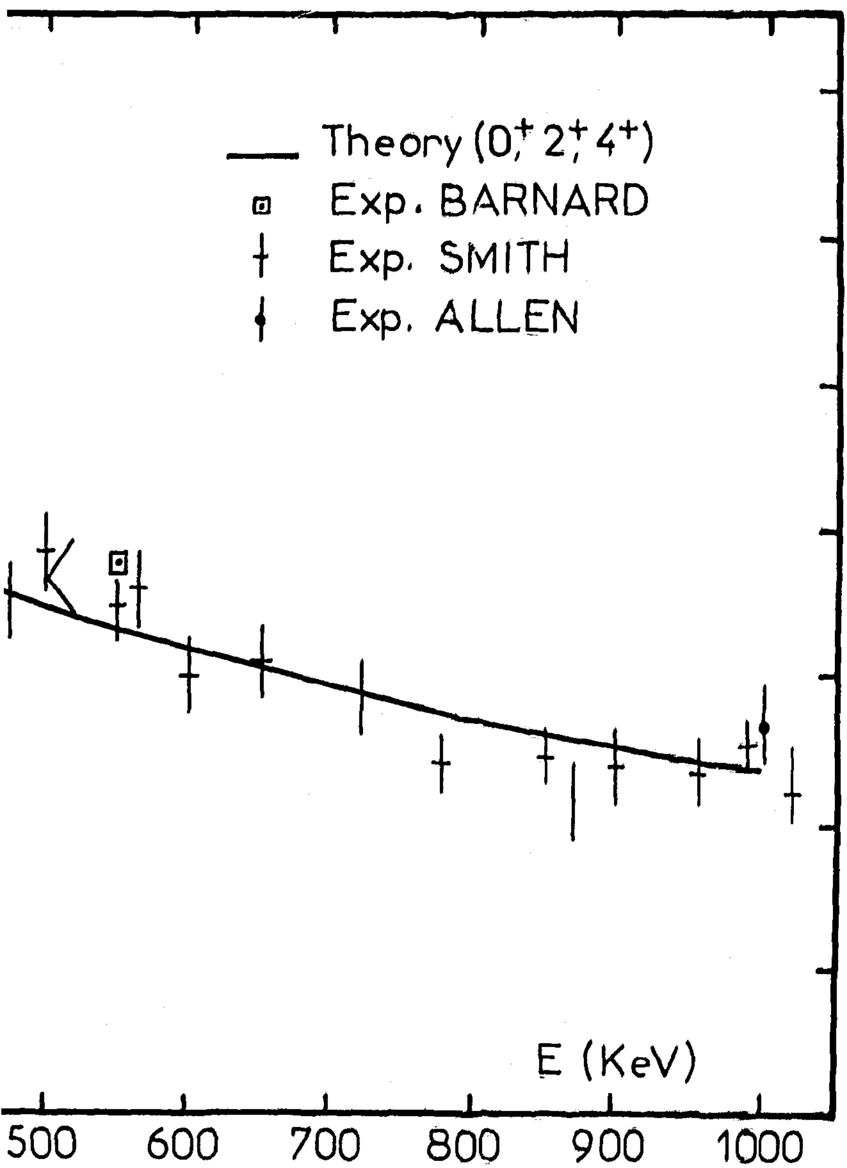
Theory ($0^+, 2^+, 4^+$)
Exp. BARNARD
Exp. SMITH
Exp. ALLEN
E (KeV)
500
600
700
800
900
1000

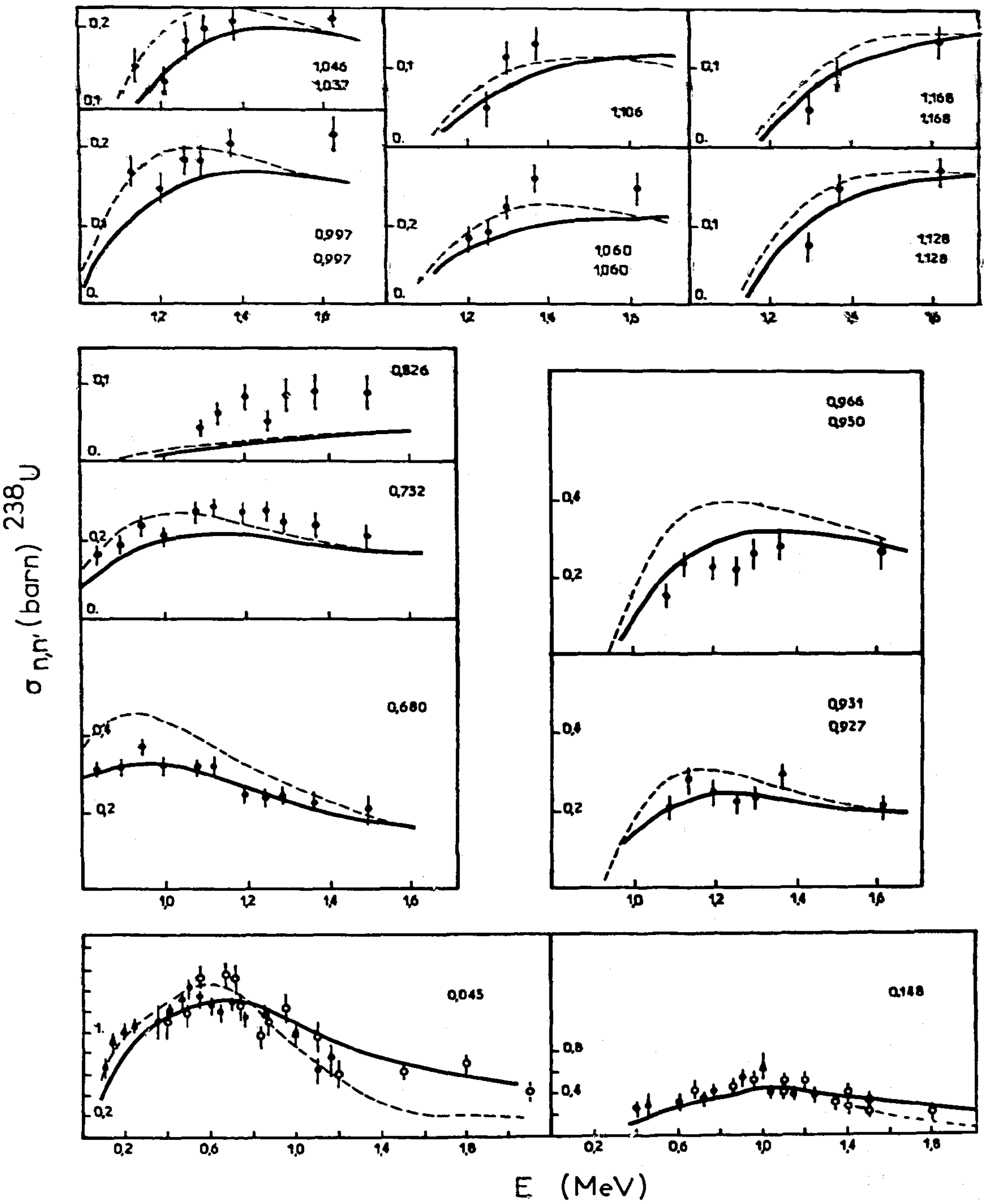
1,046
1,037
1,106
1,168
1,168
0,997
0,997
1,060
1,060
1,128
1,128
0,826
0,732
0,680
0,966
0,950
0,931
0,927
0,045
0,148
$\sigma_{n,n'}$ (barn) ^{238}U
E (MeV)

Fig. 8

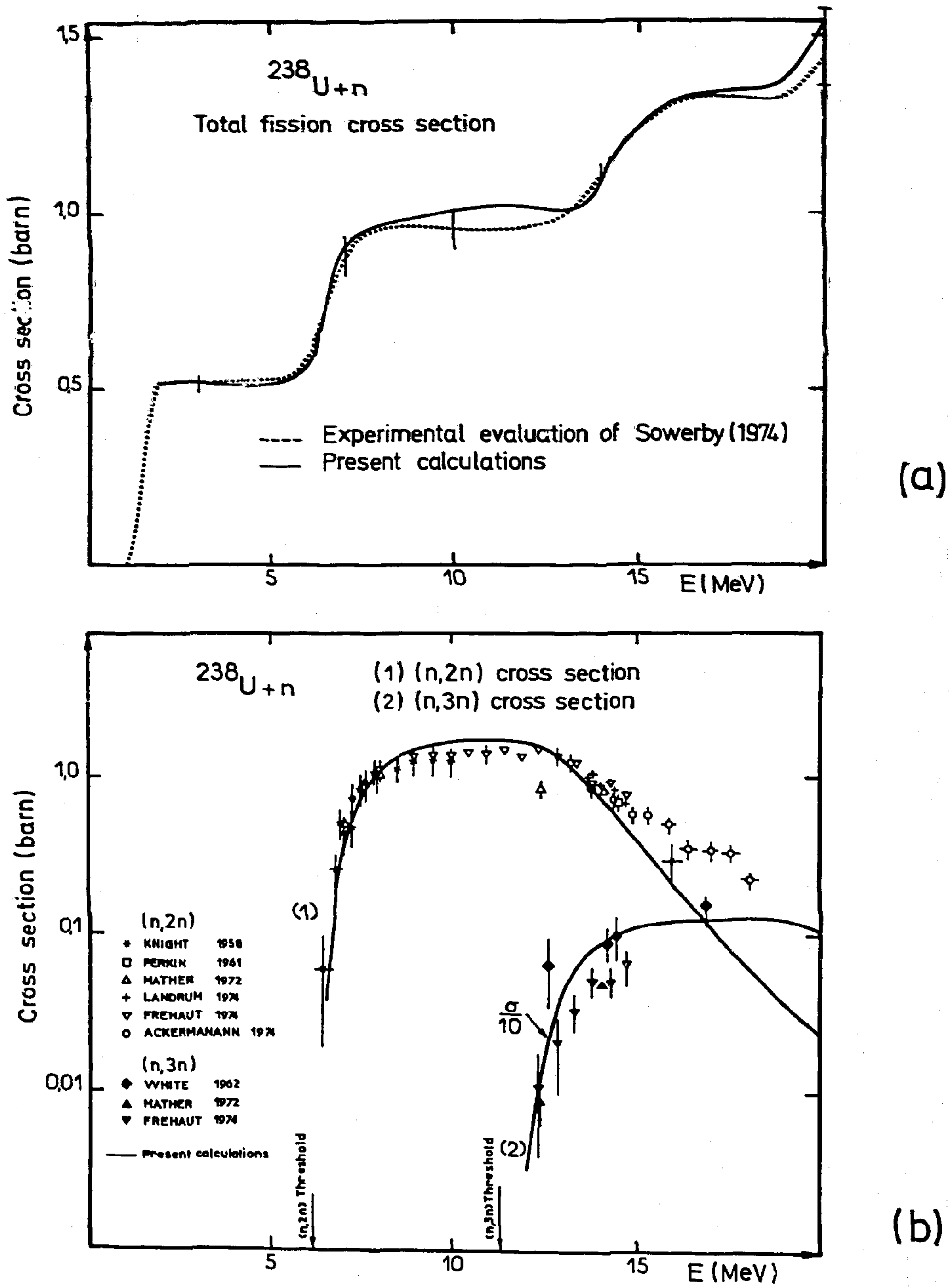

238U+n
Total fission cross section
Cross section (barn)
1,5
1,0
0,5
5
10
15
E(MeV)
---- Experimental evaluation of Sowerby (1974)
—— Present calculations
(a)
238U+n
(1) (n,2n) cross section
(2) (n,3n) cross section
Cross section (barn)
1,0
0,1
0,01
(n,2n)
KNIGHT 1958
PERKIN 1961
MATHER 1972
LANDRUM 1974
FREHAUT 1974
ACKERMANANN 1974
(n,3n)
WHITE 1962
MATHER 1972
FREHAUT 1974
Present calculations
(1)
(2)
a/10
(n,2n) Threshold
(n,3n) Threshold
5
10
15
E (MeV)
(b)

Fig. 9